ELSEVIER

Journal of Nuclear Materials 241–243 (1997) 633–638

journal of nuclear materials

The role of turbulent transport in DIII-D edge and divertor plasmas

R.A. Moyer [a,*], J.W. Cuthbertson [a], T.E. Evans [b], G.D. Porter [c], J.G. Watkins [d]

[a] *Fusion Energy Research Program, University of California, San Diego, CA 92093-0417 USA*
[b] *General Atomics, PO. Box 85608, San Diego, CA 92185-5608, USA*
[c] *Lawrence Livermore National Laboratory, Livermore, CA USA*
[d] *Sandia National Laboratories, Albuquerque, NM USA*

Abstract

Reciprocating Langmuir probes have been used to investigate turbulent transport in DIII-D edge and divertor plasmas. The turbulent particle flux on the outboard midplane exceeds the particle flux from the 2-D local transport code UEDGE by a large enough factor to allow for substantial poloidal asymmetry in the turbulent transport. Changes in the turbulent effective diffusion coefficient in the edge agree qualitatively with particle confinement changes. Potential fluctuations $e\tilde{\phi}_f/kT_e$ in the divertor in attached ELM-free conditions are comparable to $e\tilde{\phi}_f/kT_e$ on the outboard midplane. ELMs transiently enhance $e\tilde{\phi}_f/kT_e$ to 2 in attached plasmas and to 2–20 in detached plasmas. Such strong turbulence ($e\tilde{\phi}_f/kT_e > 1$) in the divertor may affect the mean energy of ions striking the divertor target plates by altering the sheath potential and therefore affect target plate erosion rates.

Keywords: DIII-D; Turbulence; Particle transport and confinement; Detached plasma

1. Introduction

In this paper we present results of electrostatic fluctuation measurements with reciprocating Langmuir probe arrays on the outboard midplane [1] and in the lower divertor [2] of the DIII-D tokamak. These results are used to evaluate the impact of electrostatic turbulence in DIII-D edge and divertor plasmas. The local turbulent particle flux across the separatrix on the outboard midplane in various confinement regimes is compared with the particle flux, obtained from a local transport analysis with the UEDGE 2-D time dependent fluid code [3], which is consistent with the global power balance and measured plasma edge gradients (n_e, T_e and T_i). First results from the lower divertor probe array ('X-point' probe) are used to evaluate potential fluctuation levels in attached and partially detached divertor plasmas, with and without ELMs.

It is generally accepted that the origin of anomalous edge particle transport in tokamaks is electrostatic turbulence-driven transport. The experimental evidence for this conclusion comes primarily from ohmic discharges in circular cross-section limiter tokamaks [4,5]. Although this is generally assumed to be true in divertor tokamaks despite differences in the edge magnetic topology and shear, and in various confinement regimes, there is little experimental evidence for this assumption. This is due, in part, to the complexity of determining the global particle balance and transport rates accurately in tokamaks with high recycling divertors [6–8]. Further complications arise when considering non-stationary discharges, including continuously evolving ELM-free H and VH-modes, and the impact of ELMs in steady-state ELMy H-modes.

2. Turbulent transport in various confinement regimes

The midplane probe array was used to measure simultaneously the boundary plasma profiles (n_e, T_e, ϕ_f) and the fluctuating quantities $\tilde{n}_e(k_\theta, \omega)$ and $\tilde{\phi}_f(k_\theta, \omega)$ at the outboard midplane across transitions from ohmic to ohmic H-mode and L to ELM-free H-mode and in ELMy H-mode and VH-mode discharges. The fluctuation-driven particle

* Corresponding author. Tel.: +1-619 455 2275; fax: +1-619 455 4156; e-mail: moyer@gav.gat.com.

PII S0022-3115(96)00578-8

flux Γ_{turb} was evaluated using $\Gamma_{turb} = \langle \tilde{n}_e \tilde{v}_r \rangle = \langle \tilde{n}_e \tilde{E}_\theta / B_t \rangle$ where $\tilde{n}_e$ is the root-mean-square (rms) electron density fluctuation amplitude, $\tilde{E}_\theta$ is the rms poloidal electric field fluctuation amplitude, B_t is the toroidal magnetic field and the $\langle\rangle$ denote an ensemble average [9]. These local measurements on the outboard midplane do not account for poloidal variations which would result from any ballooning character to the turbulence [10] and which are expected to be greatest in ohmic and L-mode plasmas [11].

To determine whether or not there are any regimes in which turbulent particle transport is unimportant in the edge, we correlate particle confinement and edge profile gradient variations with variations in the turbulence and

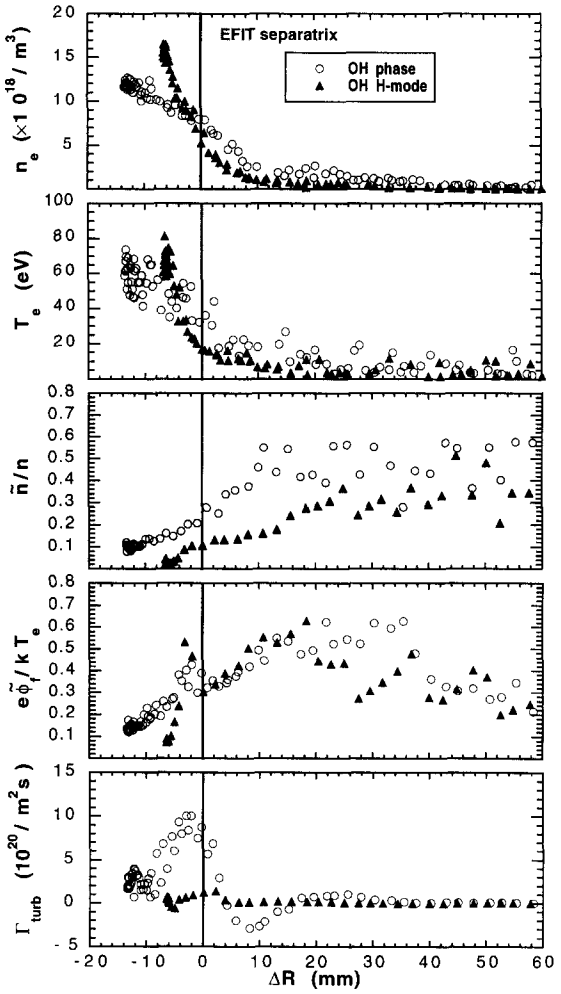

Fig. 1. Radial variation of, top to bottom, the electron density n_e and temperature T_e profiles, the rms fluctuations amplitudes $\tilde{n}_e / n_e$ and $e\tilde{\phi}_f / kT_e$ and the turbulent radial particle flux Γ_{turb} in the ohmic and ohmic H-mode portions of a single discharge. The profiles are plotted with respect to the magnetic separatrix location calculated by EFIT [13], $\Delta R = R - R_{sep}$.

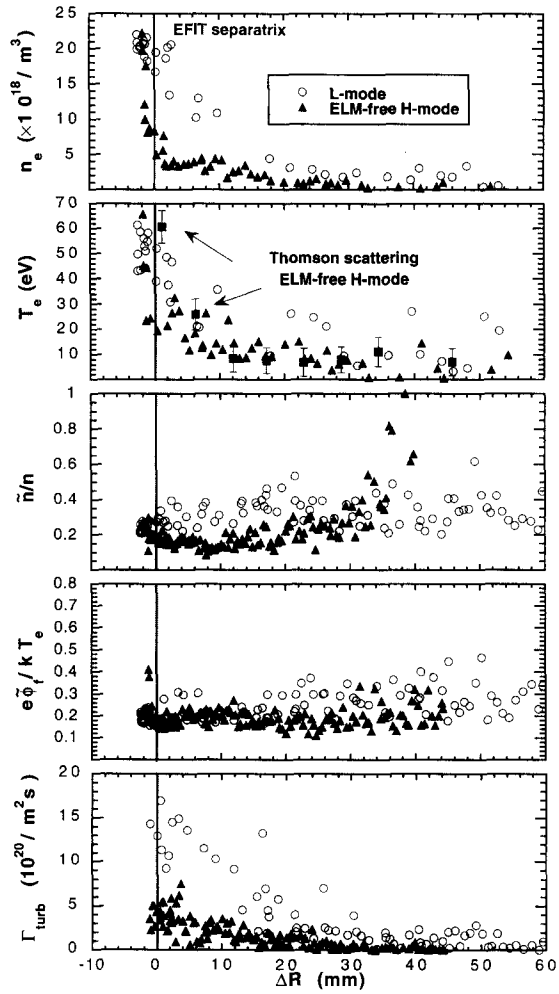

Fig. 2. Radial variation of, top to bottom, n_e, T_e, $\tilde{n}_e / n_e$, $e\tilde{\phi}_f / kT_e$ and Γ_{turb} in the L-mode and ELM-free H-mode portions of a single discharge in DIII-D.

associated transport at and just inside the separatrix. Profiles of the electron density n_e and temperature T_e, the normalized fluctuation amplitudes $\tilde{n}_e/n$ and $e\tilde{\phi}_f/kT_e$ and the turbulent particle flux Γ_{turb} are shown in Figs. 1–3 for ohmic and ohmic H-mode, L and ELM-free H-mode and ELMy H and (ELM-free) VH-mode respectively. The ELMs in H-mode (Fig. 3) were 30 ms apart, with 3 ELMs during the profile measurement. Since the I_{sat} increase during each ELM exceeded the power supply capability, data during the ELMs was removed, and the resulting profile between ELMs is plotted. Changes in the edge profile and turbulent transport parameters are summarized in Table 1.

Γ_{turb} is reduced on the outboard midplane 10 × in ohmic H-mode relative to the ohmic phase (Fig. 1). Both the n_e profile (4 ×) and the T_e profile (3 ×) steepen. This

dramatic *local* transport reduction results in large part from reductions in $\tilde{n}_e/n$ by 2 × in the SOL and up to 10 × inside separatrix, and in $e\tilde{\phi}_f/kT_e$, which remains unchanged in the scrape-off layer, but decreases up to 5 × inside the separatrix.

Within 100 ms of the L to H transition, Γ_{turb} is reduced 3–5 × in ELM-free H-mode relative to L-mode (Fig. 2). The n_e profile steepens 6–8 × and the T_e profile steepens 3 ×. $\tilde{n}_e/n$ is reduced 2–3 × in the SOL and up to separatrix, while $e\tilde{\phi}_f/kT_e$ remains unchanged.

Γ_{turb} is 5 × lower in VH-mode than in an ELMy H-mode at a similar neutral beam heating power P_{inj} with ELMs spaced 30 ms apart (Fig. 3). The VH-mode n_e profile ($P_{inj} = 3.4$ MW) is twice as narrow as the ELMy H-mode profile ($P_{inj} = 4$ MW). The n_e profile is also broader in the ELMy H-mode than the ELM-free H-mode (Fig. 2). With higher frequency ELMs, the SOL n_e and T_e profiles broaden further [12]. The $\tilde{n}_e/n$ are similar in the SOL except within 10 mm of the separatrix, where $\tilde{n}_e/n$ in the VH-mode drops sharply. In the ELMy H-mode, $e\tilde{\phi}_f/kT_e \approx 1$ across the SOL, while in the VH-mode, $e\tilde{\phi}_f/kT_e$ decreases from 1 far from the separatrix to $e\tilde{\phi}_f/kT_e \approx 0.4$ within 10 mm of the separatrix.

3. Determination of an effective turbulent diffusion coefficient

To determine if the edge particle transport is dominated by anomalous turbulent diffusion, we compare Γ_{turb} across changes in confinement regime. Since Γ_{turb} scales linearly with the local density, Γ_{turb} must be normalized before comparing values in different regimes. We normalize Γ_{turb} to the local electron density gradient ∇n_e: $D_{eff}^{turb} = \Gamma_{turb}/\nabla n_e$. This normalization creates a quantity which mimics a real transport coefficient and even in the case of non-diffusive transport (e.g. inward convective pinch), this form is equivalent to D_{eff} in the UEDGE local transport analyses. Because single exponentials provide poor fits to Γ_{turb} and $n_e(r)$, the profiles are fit with either bi-exponential or smooth, non-exponential (ohmic only) functions, retaining some radial variation in D_{eff}^{turb} to assess the impact of the uncertainty (±5 mm) in the separatrix location determined by the EFIT magnetic equilibrium code [13]. The D_{eff}^{turb} for the data in Figs. 1–3 are shown in Fig. 4. D_{eff}^{turb} correlates with changes in confinement regime: the reduction in D_{eff}^{turb} is *qualitatively* consistent with the particle confinement improvement [6,14] (Table 1). No counter-example, for which D_{eff}^{turb} changes opposite to the particle confinement changes, is found. A similar conclusion follows from comparison of Γ_{turb} to the particle fluxes in the UEDGE simulations.

Care must be taken not to over-interpret the D_{eff}^{turb} values more than 5 mm outside the separatrix since we have neglected parallel transport and the SOL particle source. In general, $D_{eff}^{turb} \approx 1$–1.5 m^2/s. Exceptions include the ohmic discharge (Fig. 4a), in which a turbulent inward pinch in the SOL (not seen in all ohmic discharges) and the particle source inside the separatrix give D_{eff}^{turb} an oscillatory structure; and the strong D_{eff}^{turb} reduction within

Table 1
Edge profile, turbulent transport and UEDGE parameters for this work. Probe quantities are evaluated at the separatrix, except ELMY H-mode and VH-mode at $\Delta R = +10$ mm. UEDGE and probe results for ELMY H and VH-modes are from different discharges. Ohmic λ_n values are from inside the separatrix (in the SOL). λ_{Te} for ELM-free H and VH-modes are from combined Thomson scattering and probe data

Confinement mode	λ_n (mm) ±1 mm	λ_{Te} (mm) ±1 mm	$\tilde{n}_e/n$	$e\tilde{\phi}_f/kT_e$	Γ_{turb} (10^{20} /m^2 s)	D_{eff}^{turb} (m^2/s)	D_{eff}^{UEDGE} (m^2/s)
Ohmic	31 (8)	13	0.2–0.3	0.3–0.4	10 ± 2	1.4 ± 1.2	
Ohmic H	7	4	0.1–0.15	0.3–0.4	1.0 ± 0.5	0.15 ± 0.06	
Oh / Oh H − mode	4.4	3.3	2–3	≈ 1	10 ± 5.4	9.3 ± 8.8	
L	17	18	0.3–0.4	0.15–0.3	15 ± 4	1.3 ± 0.52	0.15
ELM-free H	2.5	6	0.1–0.2	0.15–0.3	4 ± 1.5	0.3 ± 0.03	0.06
L / ELM − free H	6-8	3	2–3	≈ 1	3.8 ± 1.7	4.3 ± 1.8	2.5
ELMy H	10	4	0.15–0.2	0.8–1	5 ± 2	0.8 ± 0.12	0.62
VH	5	3	0.05–0.1	0.4–0.6	1 ± 0.5	0.2 ± 0.02	0.13
ELMy H / VH	2	1.3	2	2	5 ± 3.2	4 ± 0.4	4.8

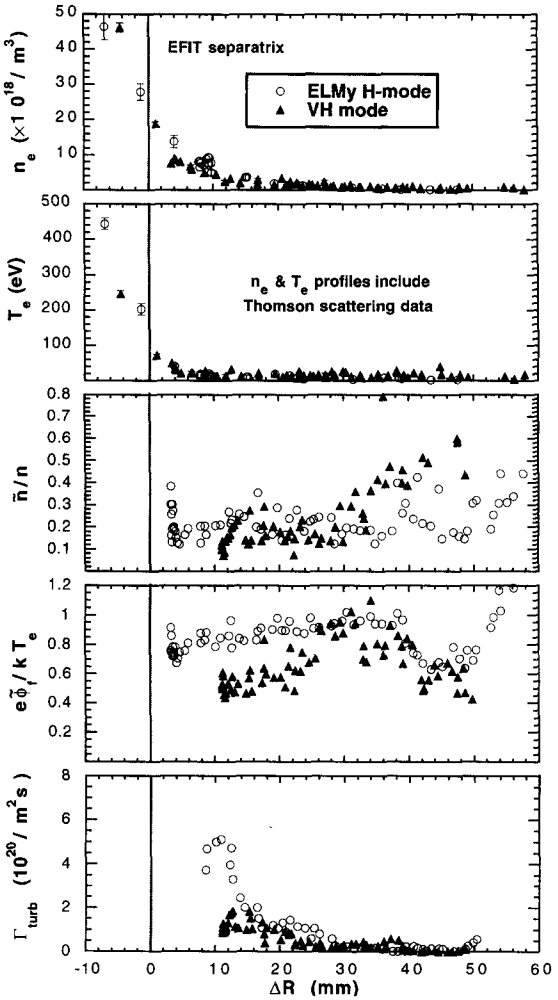

Fig. 3. Radial variation of, top to bottom, n_e, T_e, $\tilde{n}_e / n_e$, $e\tilde{\phi}_f / kT_e$ and Γ_{turb} in an ELMy H-mode and a VH-mode with similar P_{inj}. The n_e and T_e profiles include Thomson scattering and probe data.

5 mm of the separatrix in the ELM-free H-mode (Fig. 4b). This reduction suggests that the H-mode transport barrier extends into the SOL, a conclusion which has also been inferred from local transport analysis of Alcator C-Mod data [15].

4. Comparison of D_{eff}^{turb} with D_{eff} from UEDGE modeling

We have modeled the L-mode and ELM-free H-mode phases of a single discharge using the UEDGE 2-D time dependent fluid code [3]. The UEDGE simulations provide effective radial particle and heat transport coefficients D_{eff}^{UEDGE} and χ_{eff}^{UEDGE} by dividing the particle and heat fluxes across the separatrix that are consistent with the global power balance by the low-field side n_e, T_e and T_i profile gradients (measured by Thomson scattering, probe and charge exchange recombination spectroscopy). The effective transport coefficients are independent of poloidal angle and radius. The transport fluxes are poloidally asymmetric due to the Shafranov shift which compresses flux surfaces on the low field side of the torus relative to the high field side. The UEDGE code models parallel and perpendicular SOL transport and uses the measured heat flux and D_α emission profiles at the divertor target plates to constrain the simulation. The resulting D_{eff}^{UEDGE} values are included in Table 1; the corresponding χ_{eff}^{UEDGE} values are $\chi_i = \chi_e = 0.8$ m^2/s in L-mode, $\chi_i = \chi_e = 0.05$ m^2/s in ELM-free H-mode, $\chi_i = 1$ m^2/s and $\chi_e = 2.3$ m^2/s in ELMy H-mode and $\chi_i = 0.1$ m^2/s and $\chi_e = 0.85$ m^2/s in VH-mode. These coefficients are similar to those obtained for JET L and H-mode discharges with 2-D edge fluid code (EDGE2D) modeling [16] and an interpretative 'onion-skin' local transport model [17].

There is apparent agreement between D_{eff}^{turb} and D_{eff}^{UEDGE} in ELMy H and VH-modes (Table 1), although the discharges modeled [12] were not those studied with the probe, and the modeling had substantially more of the power in the ion channel than in the L-mode and ELM-free H-mode modeling [12]. The D_{eff} decrease from L to H-mode in the UEDGE simulations is a factor of 2.5; typical reductions are 2–3. These D_{eff} reductions are just

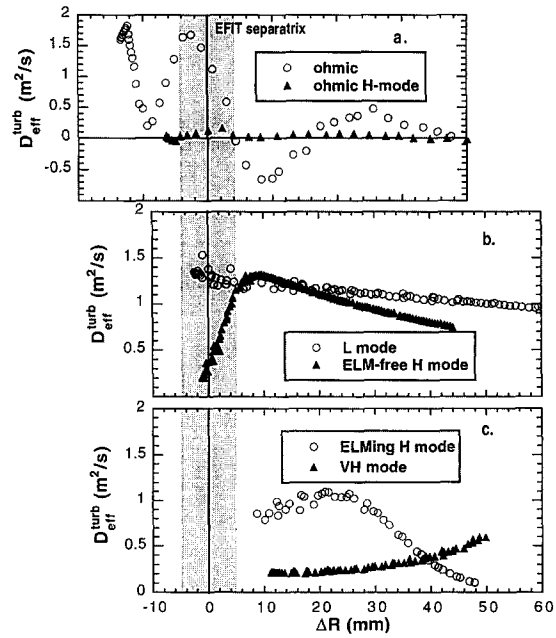

Fig. 4. Radial profiles of D_{eff}^{turb} in: (a) ohmic (○) and ohmic H-mode (▲) phases of the discharge in Fig. 1. (b) L-mode (○) and ELM-free H-mode (▲) phases of the discharge in Fig. 2. (c) ELMy H-mode (○) and ELM-free VH-mode (▲) in the discharges in Fig. 3.

within the uncertainty in the turbulent transport changes: $D_{\text{eff}}^{\text{turb}}$ drops 2.5–6.1 × (Table 1). The turbulent particle flux exceeds the outboard midplane particle flux in the UEDGE simulation by a large factor: Γ_{turb} L-mode (H-mode) = 15(4) × $10^{20}/\text{m}^2$ s ≫ Γ_{UEDGE} L-mode (H-mode) = 2.1(1.4) × $10^{20}/\text{m}^2$ s. We conclude that the turbulent particle flux on the outboard midplane exceeds the particle flux obtained from the UEDGE local transport model by a large enough factor to allow for substantial poloidal asymmetry in the turbulent transport in the L and ELM-free H-modes. An order of magnitude in/out asymmetry in DIII-D L-modes is consistent with coherent scattering measurements of density fluctuations [18] and with turbulent transport simulations [10,19]. The results suggest either decreasing poloidal asymmetry in the turbulent transport [11,20] or decreasing non-diffusive transport (an inward convective pinch) from L to H to VH-mode, consistent with helium pinch velocities measured in the core of similar discharges in helium transport studies [21]. This point requires further investigation.

5. Turbulence in divertor plasmas

Fluctuation data in the divertor are presently limited to floating potential fluctuations $\tilde{\phi}_{\text{f}}$ in the bandwidth dc $< f <$ 500 kHz. The normalized rms amplitude $e\tilde{\phi}_{\text{f}}/kT_{\text{e}}$ versus height above the divertor floor in the outer divertor leg is shown in Fig. 5a for representative attached L and ELMy H-modes. The L-mode $e\tilde{\phi}_{\text{f}}/kT_{\text{e}}$ is consistent with outboard midplane values (Table 1; Fig. 2). ELMs enhance $e\tilde{\phi}_{\text{f}}/kT_{\text{e}}$ both at the midplane (≈ 1 steady state) and in the divertor, where the individual ELMs drive $e\tilde{\phi}_{\text{f}}/kT_{\text{e}}$ transiently to 1–2. In partially detached divertor (PDD) operation, $e\tilde{\phi}_{\text{f}}/kT_{\text{e}}$ in the outer divertor leg during ELMs can reach 2–12 (Fig. 5b), due in part to the T_{e} reduction at detachment. Due to a systematic difference between T_{e} measured with the swept double probe (T_{e} = 4–5 eV) and the divertor Thomson scattering system (T_{e} = 1–2 eV) in PDD discharges, these enhancement factors are lower limits. This large potential fluctuation amplitude, in PDD conditions where $T_{\text{i}} \approx T_{\text{e}} \leq$ 1–2 eV [22], can increase target plate erosion since it contributes to the mean ion energy by enhancing the sheath potential $e\phi_{\text{sh}} \approx 3kT_{\text{e}}$. This enhancement is especially critical for high Z metals, since it could raise the mean ion energy above the threshold for sputtering these materials. Enhancement of the mean ion energy due to potential fluctuations (driven by applied rf) has been reported for a helicon wave source plasma [23]. Preliminary comparison of net carbon erosion rates at the outer divertor strike point with DiMES in ELM-free and ELMy H-modes suggest that erosion is enhanced in ELMy discharges beyond that expected due to changes in the quiescent heat flux [24]. Measurements in disruptive discharges of charge exchange neutral energy distributions at the divertor floor in the private flux region by deuterium

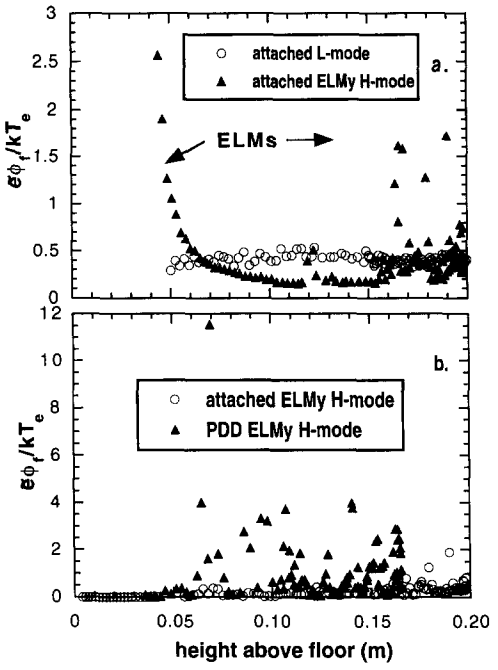

Fig. 5. $e\tilde{\phi}_{\text{f}}/kT_{\text{e}}$ versus height above the floor in the outer divertor leg in (a) attached L-mode (○) and ELMy H-mode (▲) discharges and (b) in attached ELMy H-mode (○) and a PDD ELMy H-mode (▲).

depth profiling of an exposed silicon wafer [25] suggest that a significant population (well above a Maxwellian distribution) of ions with energies well above the average incident energy are present, but may not be generally true.

6. Summary

The turbulent particle flux on the outboard midplane exceeds the particle flux from a local transport model (UEDGE) by a large enough factor to allow for substantial poloidal asymmetry in the turbulent transport. On the outboard midplane, Γ_{turb} exceeds Γ_{UEDGE} by 11 in L-mode and 2.4 in ELM-free H-mode and exceeds the *flux surface averaged* particle flux in UEDGE by 18 (L-mode) and 4.5 (ELM-free H-mode). The changes in $D_{\text{eff}}^{\text{turb}}$ agree qualitatively with particle confinement changes. Comparison of Γ_{turb} with Γ_{UEDGE} in the sequence L to ELM-free H to ELMy H and VH-mode suggests either decreasing poloidal asymmetry in turbulent transport as expected for an edge E_{r} shear layer, or decreasing inward convective transport, as measured for helium transport in similar discharges.

In attached, ELM-free conditions, $e\tilde{\phi}_{\text{f}}/kT_{\text{e}}$ in the outer divertor leg is comparable to $e\tilde{\phi}_{\text{f}}/kT_{\text{e}}$ on the outboard midplane. ELMs transiently enhance $e\tilde{\phi}_{\text{f}}/kT_{\text{e}}$ to 2 in attached divertor plasmas and as high as 2–12 in detached

conditions. Such strong turbulence ($e\tilde{\phi}_f/kT_e > 1$) in the divertor may affect the mean energy of ions striking the divertor target plates by altering the sheath potential and therefore affect target plate erosion rates.

Acknowledgements

Work supported by U.S. Department of Energy under Grant DE-FG03-95ER54294 and Contract Nos. DE-AC03-89ER5114, DE-AC04-94AL85000 and W-7405-ENG-48.

References

[1] J.G. Watkins et al., Rev. Sci. Instrum. 63 (1992) 4728.
[2] J.G. Watkins et al., Rev. Sci. Instrum. (1996) in press.
[3] T. Rognlien et al., J. Nucl. Mater. 196–198 (1992) 347.
[4] W.L. Rowan et al., Nucl. Fusion 27 (1987) 1105.
[5] C.P. Ritz et al., Phys. Rev. Lett. 62 (1989) 1844.
[6] M.E. Rensink et al., Phys. Fluids B 5 (1993) 2165.
[7] W.L. Rowan et al., J. Nucl. Mater. 220–222 (1995) 668.
[8] M.E. Fenstermacher et al., J. Nucl. Mater. 220–222 (1995) 330.
[9] R.A. Moyer et al., J. Nucl. Mater. 196–198 (1992) 854.
[10] P.N. Guzdar and A.B. Hassam, Phys. Plasmas (1996) submitted.
[11] G.R. Tynan et al., in: Int. Topical Conf. on New Ideas in Tokamak Confinement, La Jolla, CA (American Institute of Physics, 1992).
[12] R.A. Jong et al., Plasma Phys. Control. Fusion 38 (1996) 1381.
[13] L.L. Lao et al., Nucl. Fusion 25 (1985) 1611.
[14] G.L. Jackson et al., J. Nucl. Mater. 220–222 (1995) 173.
[15] B. LaBombard et al., these Proceedings, p. 149.
[16] A. Loarte et al., J. Nucl. Mater. 220–222 (1995) 606.
[17] R.D. Monk, et al., J. Nucl. Mater. 220–222 (1995) 612–616.
[18] C.L. Rettig, private communication (1996).
[19] R.E. Waltz et al., Phys. Plasmas 1 (1994) 2229.
[20] T.L. Rhodes et al., Nucl. Fusion 33 (1993) 1787.
[21] M.R. Wade et al., in: Eur. Conf. on Controlled Fusion and Plasma Physics, Kiev (European Physical Society, 1996).
[22] R. Isler et al., Phys. Plasmas (1996) in press.
[23] J.-H. Kim and H.-Y. Chang, Phys. Plasmas 3 (1996) 1462.
[24] D. Whyte et al., these Proceedings, p. 660.
[25] R. Bastasz et al., these Proceedings, p. 650.